The Bioactive Polypyrrole/Polydopamine Nanowire Coating with Enhanced Osteogenic Differentiation Ability with Electrical Stimulation

Yuan He [1], Lingfeng Dai [1,2], Xiuming Zhang [1], Yanan Sun [1], Wei Shi [1,*] and Dongtao Ge [1,*]

[1] Department of Biomaterials, College of Materials, Xiamen University, Xiamen 361005, China; 20720140153722@stu.xmu.edu.cn (Y.H.); dlf@fjirsm.ac.cn (L.D.); zhangxiuming@xmu.edu.cn (X.Z.); sunyanan@xmu.edu.cn (Y.S.)
[2] Quanzhou Institute of Equipment Manufacturing Haixi Institutes, Chinese Academy of Science, Quanzhou 362000, China
*   Correspondence: shiwei@xmu.edu.cn (W.S.); gedt@xmu.edu.cn (D.G.)

Abstract: Polypyrrole (PPy) is a promising conducting polymer in bone regeneration; however, due to the biological inertia of the PPy surface, it has poor cell affinity and bioactivity. Based on the excellent adhesion capacity, biocompatibility, and bioactivity of polydopamine (PDA), the PDA is used as a functional coating in tissue repair and regeneration. Herein, we used a two-step method to construct a functional conductive coating of polypyrrole/polydopamine (PPy/PDA) nanocomposite for bone regeneration. PPy nanowires (NWs) are used as the morphologic support layer, and a layer of highly bioactive PDA is introduced on the surface of PPy NWs by solution oxidation. By controlling the depositing time of PDA within 5 h, the damage of nano morphology and conductivity of the PPy NWs caused by the coverage of PDA deposition layer can be effectively avoided, and the thin PDA layer also significantly improve the hydrophilicity, adhesion, and biological activity of PPy NWs coating. The PPy/PDA NWs coating performs better biocombaitibility and bioactivity than pure PPy NWs and PDA, and has benefits for the adhesion, proliferation, and osteogenic differentiation of MC3T3-E1 cells cultured on the surface. In addition, PPy/PDA NWs can significantly promote the osteogenesis of MC3T3-E1 in combination with micro galvanostatic electrical stimulation (ES).

Keywords: PPy/PDA nanocomposite; nanowires; polydopamine; electrical stimulation

1. Introduction

Conducting polymers (CPs) especially polypyrrole (PPy) with excellent conductivity, long-term stability and biocompatibility have been widely applied in many fields [1–3]. In particular, the conductivity of CPs enables their use as sensors [4], controlled drug release [5,6], and functional tissue repair materials [7,8]. Moreover, CPs with nano morphology, which mimics the natural morphology of the extracellular matrix (ECM), can be easily fabricated via electrochemical and chemical polymerization on various substrates, and makes it an outstanding coating used in the biomedical field [9,10]. Actually, many studies confirmed that the PPy applied with electrical stimulation (ES) could promote the expression of proliferation and differentiation for tissue regeneration such as bone and nerves [11–13]. However, PPy does not display functional groups to help it adhere to surfaces [14]; therefore, generating composite materials with PPy and other adhesive polymers can effectively enhance the functionality of PPy-containing coatings.

Polydopamine (PDA) could be synthesized by the self-oxidative polymerization of dopamine (DA), which is the most abundant catecholamine neurotransmitter in the brain. PDA has excellent biocompatibility and biological activity [15]. The rich functional groups, especially the catechol

compounds, offers PDA astonishing adhesive ability on a variety of materials [16,17]. Many studies focusing on the use of PDA as a surface functional modification material to improve the biocompatibility and surface modifiability of other materials were reported [18]. However, the PDA has poor conductivity without electrical signal response. Moreover, the inescapable fact is that the oxidative polymerization of dopamine (DA) is uncontrollable, which means it is very difficult to control the morphology [19,20], and the condition for preparing the PDA coating with nano morphology is quite harsh.

At present, many researchers are attentive to the preparation of PPy/PDA composites, which can solve the drawbacks of the above-mentioned materials. This kind of composites can be fabricated via one-pot or two-step method to avoid the disadvantages of pure PPy and PDA [21–24]. By controlling reaction conditions, the pyrrole (PY) and DA composite material has both good morphology, conductivity, and bioactivity. Zhao et al. have demonstrated that the copolymer of DA-PPy performs improved water dispersibility, improved electrical conductivity and film adhesion than pure PPy [17,25]. Electrochemical method has more advantages than chemical polymerization in the preparation of nanostructured conducting coatings with better controllability and uniformity of thickness and morphology. By precise regulating the concentration of PY and DA, PDA/PPy composite coatings with nanowires and vesicular structure morphology with enhanced conductivity, adhesion and cell affinity have been successfully prepared via a one-pot electrochemical polymerization [26–28]. In the one-pot reaction system of PY and DA, the concentration of PY and DA both have obvious effects on the morphology and conductivity of the copolymer. The concentration of dopamine and the polymerization potential need to be precisely controlled in order to obtain the copolymer with nano morphology. Compared with the co-polymerization of PPy/PDA, the reaction condition for preparing PPy/PDA composite coatings by a two-step method is relatively simple, as for the reaction condition of preparation pure PPy coating with various nano structure and size morphology can be controlled more easily and precisely by electrochemical deposition [29,30]. However, in order to better control the morphology and conductivity of the products, the most reported study on preparation of PPy/PDA composites via a two-step method is always setting fabrication of PPy layer as the final step to ensure the excellent conductivity [23,31]. Taking the PDA as the outer layer is more beneficial to improve the biocompatibility of PPy/PDA composites, and the key point is to precisely control the thickness of PDA deposition. The best result is that the deposition of PDA on the surface of PPy NWs will not significantly change the nano morphology of the first layer, nor reduce the conductivity.

In this study, the PDA modified PPy/PDA nanowire (NW) coating is synthesized by a two-step reaction (Figure 1). The first layer is preparation PPy NWs coating by electrochemical polymerization as the template, and the PDA layer is following deposited on each PPy NWs surface by solution oxidation. By regulating the deposition time of PDA, the influence of different PDA depositing time on the conductivity of PPY/PDA NWs coating is studied, and the optimal PDA deposition time is determined. The morphology, chemical structure, hydrophilicity, adhesiveness are further characterized. The cell affinity and bioactivity of the PPy/PDA NWs coating on MC3T3-E1 cell are further evaluated. The PPy/PDA NWs coating provides enhanced hydrophilicity and adhesiveness. The introduced PDA layer indeed improves the cell adhesion, proliferation, and differentiation of MC3T3-E1. Combined with ES, the PPy/PDA NWs coating shows better osteogenic activity to accelerate maturation of MC3T3-E1 cells.
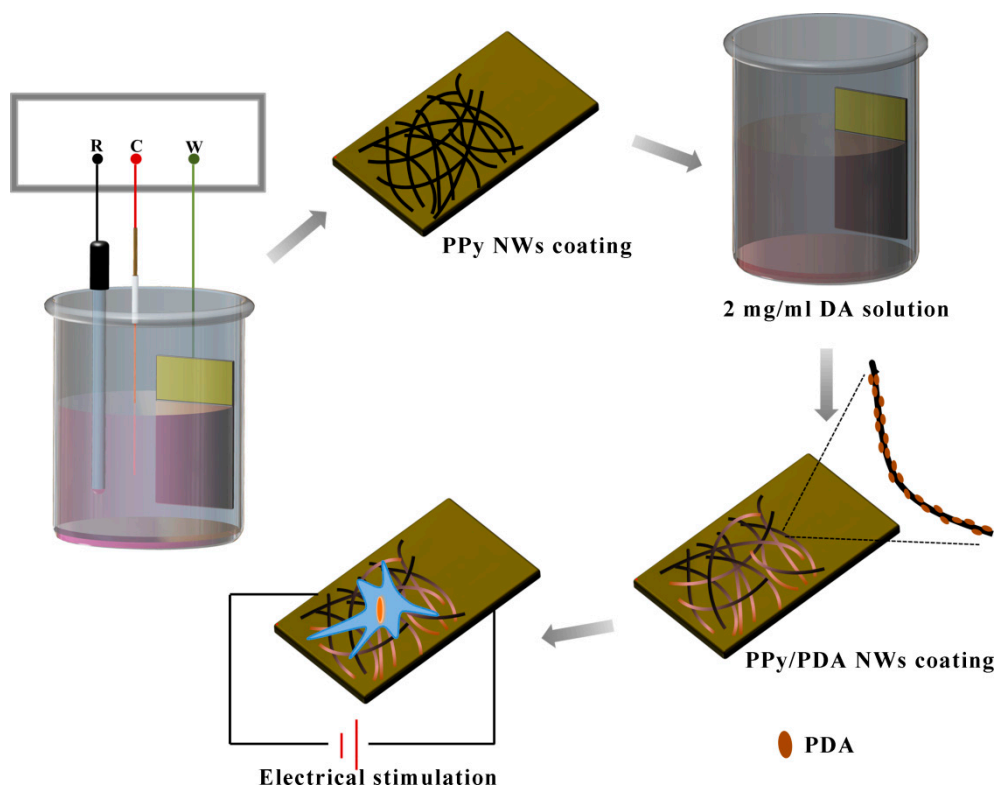
Figure 1. Illustration of preparation of PPy/PDA NWs coating and the synergistic effect with electrical stimulation on MC3T3-E1.

2. Materials and Methods

2.1. Materials

Pyrrole (PY, 98%) and sodium p-toluenesulfonate were purchased from J & K Chemical Ltd. (Beijing, China) Dopamine hydrochloride (98%), Vitamin C and β-glycerophosphate were bought from Sigma-Aldrich (Shanghai, China). Tris(dydroxymethyl) aminomethane (Tris-HCl, 99%) was purchased from Sangon Biotech Co. Ltd. (Shanghai, China). Other used inorganic salt reagents such as sodium chloride (NaCl), potassium chloride (KCl), disodium hydrogen phosphate (Na_2HPO_4), sodium dihydrogen phosphate (NaH_2PO_4), hydrochloric acid (HCl) were bought from SINOPHARM (Beijing, China). Monocrystal silicon wafer (p-type, 0.5 mm) was taken from Xiamen Zhongli Technology Co. Ltd. (Xiamen, China).

Before used, pyrrole need to be purified by distillation under the protection of N_2 gas and stored in the refrigerator at −20 °C for future use. Other reagents can be used directly without additional treatment. The water used in experiments was ultrapure water (18.2 MΩ).

Monocrystal silicon wafers were first cleaned via boiled in Piranha solution (H_2SO_4:H_2O_2 = 4:1) for 15 min and washed in hot water, then dried by nitrogen for further use. Next, a 500 nm thick of oxide layer was formed on the silicon surface by thermal diffusion oxidation. Finally, 50 nm titanium and 100 nm gold layer were fabricated in the silicon wafer surface via magnetron sputter. The Au/Ti/Si wafer was diced for further experiment.

2.2. Synthesis of PPy/PDA Nanowires (NWs) Coating

The PPy/PDA NWs coating was fabricated via a two-step method. In brief, the first step was the polymerization of PPy NWs layer by electrochemical deposition, and the second step was the deposition of PDA layer on the surfaces of PPy NWs via solution oxidation.

First, Pyrrole monomers could be polymerized with proper oxidation potential to form PPy. In this manuscript, the PPy NWs coating was directly fabricated by electrochemical polymerized on the Au/Ti/Si wafer under a potential at 0.8 V for 200 s with CHI660D electrochemical workstation (Chen Hua Instrument Company, Shanghai, China). The electropolymerization process of pyrrole was carried out in a traditional three-electrode system, in which the Au/Ti/Si wafer was the working electrode, a platinum wire was the counter electrode and a saturated calomel electrode (SCE, INESA Scientific Instrument Co. Ltd., Shanghai, China) was the reference electrode. The pyrrole monomer was dissolved in the electrolyte of 0.2 M PBS solution (pH = 7.4) containing 0.14 M of pyrrole and 0.085 M sodium p-toluenesulfonate. After 200 s, a uniform layer of PPy NWs can be deposited on the surface of the Au/Ti/Si substrate.

Second, the PDA layer was directly deposited on the PPy NWs by immersing the PPy NWs substrate into the fresh 2 mg/mL DA alkaline Tris-HCl solution (10 mM, pH = 8.50). The whole reaction vessel was opened and standing at room temperature for 5 h. Finally, the PPy/PDA NWs coated substrate was fished out and cleaned with distilled water.

The pure PPy NWs coating was fabricated by electrochemical polymerized the same as the first step. The Pure PDA coating was obtained on Au/Ti/Si substrate by direct immersing the bare Au/Ti/Si substrate in the fresh 2 mg/mL DA alkaline Tris-HCl solution (10 mM, pH = 8.50) for 5 h. The fabricated PPy/PDA NWs, PPy NWs, and PDA coatings were carefully washed with distilled water and dried in vacuum at 50 °C for further use.

2.3. Characterization

The morphologies of PPy NWs and PPy/PDA NWs were observed by scanning electron microscopy (SEM, SU-70, Hitachi, Tokyo, Japan) at an accelerating voltage of 10.0 kV and transmission electron microscopy (TEM, JME-2100, JEOL, Tokyo, Japan) under 200 kV accelerating voltage. The chemical composition of pure PDA, PPy, and PPy/PDA were characterized by Fourier transform infrared spectroscopy (FTIR, Nicolet IN10, Thermo Scientific, Waltham, MA, USA) with potassium bromide (KBr) tablet method. The static contact angle of different coating samples was measured by a contact angle meter (JC2000A, Shanghai Zhongchen digital technic apparatus Co. Ltd, Shanghai, China) with 2 μL water dropped at five different positions for each sample. Each sample randomly tested three parallel specimen. The electrical conductivity of the PPy and PPy/PDA NWs coatings was evaluated by a four-point probe apparatus (SZ83, Suzhou Baishen Technology Co. Ltd, Suzhou, China). Adhesion ability of PPy NWs and PPy/PDA NWs coating with the substrate was tested with ScotchTM MagicTM Tape 810 (3M, Saint Paul, MN, USA) and each sample was repeated three times in the same direction. Cyclic voltammetry (CV) was conducted in the 0.9% NaCl solution with a CHI660D electrochemical workstation. The voltage test ranging from −0.9–0.5 V at the scan rate of 10 mV/s.

2.4. Cell Culture

The mouse embryonic osteoblast precursor cells (MC3T3-E1) was bought at the Wuhan Cell Bank of Chinese Academy of Sciences Basic Science Cell Center. MC3T3-E1 cells were cultured in the alpha-modified minimum essential medium (α-MEM, Gibco, Waltham, MA, USA) supplemented with 10% FBS (Gibco, Waltham, MA, USA) and 1% penicillin and streptomycin (Hyclone, Chicago, IL, USA) in the saturated humidity incubator with 5% CO_2 at 37 °C. During the normal subculture of cells, the medium was changed every two days.

2.5. Effect of Surface Morphology on MC3T3-E1 Adhesion and Proliferation and Differentiation

Three different morphology substrates including PPy NWs, PDA and PPy/PDA NWs coatings on Au/Ti/Si wafers and bare Au/Ti/Si wafers were first sterilized by soaking in 75% ethanol for 24 h and following immersing in distilled water for another 24 h. The bare Au/Ti/Si wafer was the control group. Before the experiment, all substrates were further irradiated under UV radiation for another 2 h.

The sterilized substrates with different morphology were placed in the 24-well plate and washed with PBS. Then 1 mL of MC3T3-E1 (2×10^4 cells/mL) suspension was seeded to each well and then cultured in cell incubator (5% CO_2, 37 °C).

2.5.1. MTT Test

To test the adhesion and proliferation ability of MC3T3-E1 cell on different substrates, the MTT assay was used to evaluate the cell viability after cells were seeded and cultured for 4, 6, 8, 12, 24, and 48 h, respectively. In brief, at the tested time point, the cell culture was carefully removed and washed with PBS twice. 500 μL fresh culture medium containing 10% MTT working solution (5 mg/mL) was added to each well and continued to incubate for another 4 h. Next, the working solution was completely removed and incubated with 500 μL DMSO to dissolve the formazan crystal under 37 °C. Finally, the optical density was tested at 570 nm using a Microplate reader (Infinity 200 pro, Tecan, Männedorf, Switzerland). Each sample was set four-parallel experiments.

2.5.2. Cell Morphology

The cell morphology of adhesion and proliferation was observed via Fluorescence microscope (Leica DM2500, Leica Camera, Wetzlar, Germany). By staining the filamentous actin (F-actin) of the MC3T3-E1 cytoskeleton, the cell spreading morphology on substrates could be observed. Generally, after MC3T3-E1 cells were cultured for 12 and 24 h, cells were rinsed with PBS and then fixed with 4% paraformaldehyde solution for 15 min. After washed with PBS, cells were continued treated with 0.1% TritonX-100 solution to enhance the permeability of cell membrane. Next, the cell was incubated in 1% BSA solution for 20 min and washed with PBS. Followed above treatments, cells were finally stained with 5 U/mL Alexa Fluor 568 phalloidin solution for 30 min in the dark environment. Samples were observed by using a fluorescence microscope.

The morphology of MC3T3-E1 cell on different substrates was further watched with SEM. After cultured for 12 h, cells were fixed and dehydrated with gradient ethanol successively. After drying, samples were sputter-coated with gold before SEM testing.

2.5.3. Total Protein Content and Alkaline Phosphatase Activity

The MC3T3-E1 cell proliferation and differentiation activities were further measured by testing the total protein content and alkaline phosphatase (ALP) activity in the period of cell proliferation and differentiation. After MC3T3-E1 cell was seeded and cultured on different substrates for 24 h, the culture medium was changed to induced medium, which additionally added 1% Vitamin C (5 mg/mL) and β-glycerophosphate (1 M). The cells were cultured normally and the fresh induced medium was changed every 2 days.

The total protein content and ALP activity were tested at 3, 7 and 14 d. At each time point, cells in each group were washed with PBS and lysed on ice by incubation with 0.1% TritonX-100-PMSF pyrolysis liquid for 3 min, then centrifuged at 4 °C for 10 min. The supernatant was collected for further protein content and ALP activity detections. Total protein content measured by using a commercial BCA protein Assay Reagen Kit (Beyotime Institute of Biotechnology, Shanghai, China) and tested absorption signal at 562 nm. The ALP activity was tested using the commercial ALP Assay Kit (Beyotime Institute of Biotechnology, Shanghai, China), and measured the absorption intensity at 405 nm. Each sample was set four-parallel experiments.

2.6. Effect of Electrical Stimulation on MC3T3-E1 Adhesion and Proliferation and Differentiation

Micro constant current electrical stimulation signal (10 μA) was directly applied on the surface of different substrates (PPy NWs and PPy/PDA NWs) via an electrochemical workstation. ES was applied from the 12 h after cells inoculation and lasted for 2 h per day for 14 days. The cell proliferation and mineralization activity detection were the same as described in the above part.

2.7. Statistical Analysis

Quantitative results were presented as mean ± standard deviation. Statistical differences among groups were analyzed by ANOVA followed by Turkey's posttest. $p < 0.05$ was considered a significant difference and represented by *, and $p < 0.01$ was considered a highly significant difference and represented by #.

3. Results and Discussion

3.1. Characterization of PPy/PDA NWs

The PPy/PDA NWs was fabricated via a two-step method. First, PPy NWs coating was electrochemical polymerized on the surface of Au/Ti/Si wafer. Under the constant voltage of 0.8 V, after 200 s, the gold electrode surface could be covered with a layer of black PPy coating completely without revealing the color of the substrate, which mean the PPy coating could effectively cover the substrate with sufficient thickness. SEM images further showed the detailed morphology of obtained PPy NWs (Figure 2a). The PPy coating had nanowire morphology. PPy NWs were slender and uniform, and tightly wound with each other. The high magnification SEM and TEM images (Figure 2c,e) detailed showed the structure of PPy NWs, the surface of PPy NWs was smooth with a diameter of about 40–60 nm. Next, after immersing PPy NWs coating into the fresh dopamine (DA) alkaline solution for several hours, a layer of PDA could be formed on PPy NWs. The PDA coated PPy NWs composites retained the former nanowire morphology with uniform size (Figure 2b,d). While compared with pure PPy NWs, the surface roughness of PPy/PDA nanowires increased, and the PDA protrusion structure adhered to the surface of PPy nanowire could be observed clearly by TEM image (Figure 2f). At the same time, the diameter of PPy/PDA NWs also increased to about 80–100 nm, indicating that PDA could be successfully polymerized on the surface of each single PPy nanowire, and the PPy/PDA had core-shell structure.

PPy has excellent electrical conductivity and electrochemical activity. Many studies were conducted to prepare responsive coatings with electrical conductivity based on the electrical conductivity of PPy. As a bioactive material, PDA can significantly improve the bioactivity of the composite. However, PDA has poor conductivity. In alkaline solution, the thickness of PDA increases with the reaction, and after reacted for 24 h, the thickness of PDA could reach above 50 nm [32]. In addition, an excessively thick layer of PDA deposition covered on PPy NWs not only concealed the nano-scale morphology of PPy/PDA composite, but also significantly reduced the conductivity of the material. Therefore, it was very important to control the depositing thickness of PDA effectively on PPy NWs surface in order to ensure the maximum retention of excellent nano morphology and conductivity. As Figure 3 indicated, by controlling the PDA depositing time, the morphology and conductivity of the PPy/PDA nanocomposite performed regular changes. Within 5 h of PDA polymerization, the morphology of the PPy NWs could be well maintained and no obvious PDA aggregates were observed. With the prolongation of deposition time, a large number of PDA random aggregates were adhered on the surface of PPy NWs. When the deposition time prolonged to 15 h, PDA particles even filled into the gap of PPy NWs, and the nanostructure morphology was gradually disappeared. At 20 h, PDA almost completely covered the whole PPy NWs coating (Figure 3a). At the same time, the conductivity change of PPy/PDA coating also displayed cliff fall after deposition time above 5 h (Figure 3b). Therefore, the deposition time of PDA was chosen at 5 h. Under this condition, the PPy/PDA nanocomposite coating could retain both good nanowire morphology and conductivity (about 1 S·cm^{-1}).
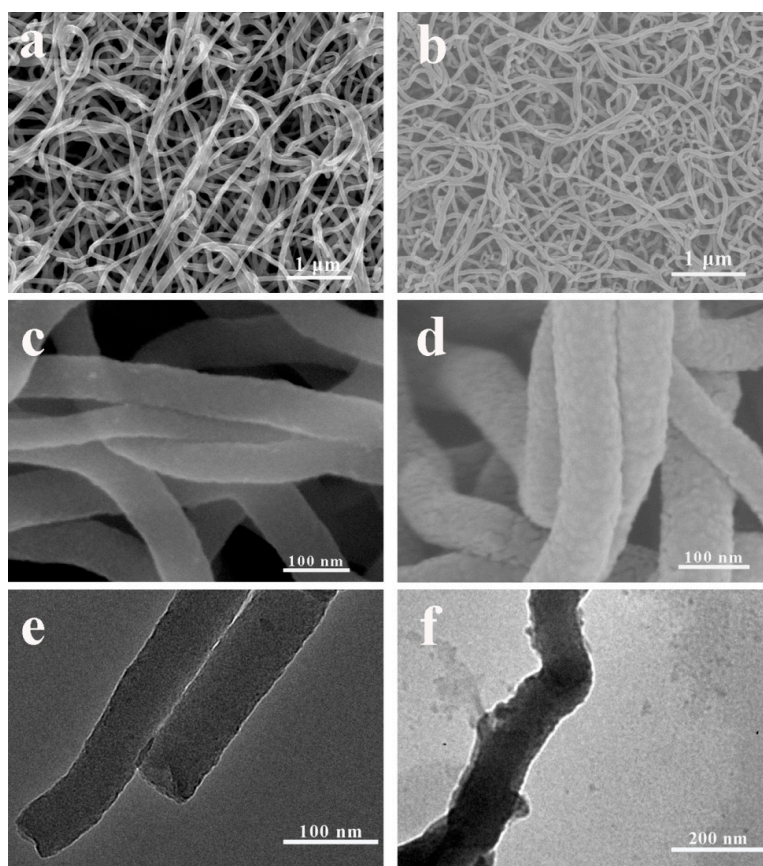
Figure 2. SEM images of PPy NWs (**a**) and PPy/PDA NWs (**b**). High resolution SEM images of PPy NWs (**c**) and PPy/PDA NWs (**d**). TEM images of PPy NWs (**e**) and PPy/PDA NWs (**f**).
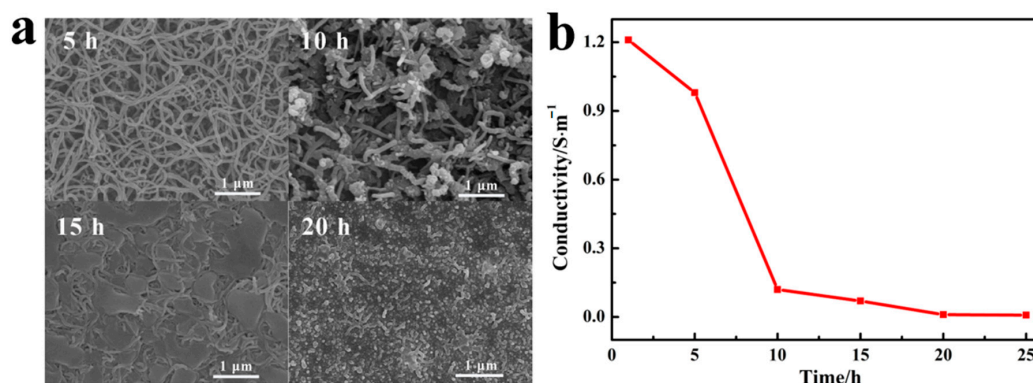

Figure 3. (**a**) SEM images of PPy/PDA NWs with different deposition time of PDA. (**b**) The conductivity of PPy/PDA NWs with different deposition time of PDA.

Comparing the FTIR spectra of pure PDA, PPy and PPy/PDA nanocomposite, it could be seen that the PPy/PDA nanocomposite possessed characteristic peaks of both pure PDA and PPy (Figure 4a): the broad peak around 3400 cm^{-1} was belonging to the N–H and O–H stretching vibrations, where PDA and PPy both have a broad peak. The peak at 1544 cm^{-1} was the characteristic peak of PPy attributed to the symmetric stretching vibrations of pyrrole ring [33]; and the characteristic peaks of PDA at 1615 and 1488 cm^{-1} ascribing to C=C and C=N/N–H stretching vibrations in aromatic amine species were also appeared [34,35], which further indicated the PDA was successfully deposited on the surface of PPy NWs to form a composite structure. Furthermore, the change of element proportion could also prove the successful modification of PDA by XPS analysis (Figure 4b). PY and DA monomers have

the same elemental composition, but there is a significant difference in the N/C ratio between PY and DA. PY (1:4) has higher theoretical N/C ratio than that of DA (1:8). After polymerization, it could be seen that the N/C ratio of PPy NWs coating (0.164) was higher than that of pure PDA coating (0.094). In addition, after PDA deposited, the N/C ratio in PPy/PDA NWs coating decreased to 0.14, which further demonstrated that PDA was successfully deposited on the surface of PPy NWs.

PDA had better hydrophilicity than PPy due to rich hydrophilic groups. The contact angle measurement displayed the change of surface hydrophilicity after PDA deposition (Figure 4c). For the bare Au surface, it had large hydrophobicity, which the average contact angle was more than 90°. After the Au surface was covered by PPy NWs or pure PDA, the water contact angle decreased more than 30°, and nanowire morphology was more conducive to the decrease of contact angle. The PPy/PDA NWs coating had the minimum water contact angle, which was only 16°. The excellent hydrophilicity of PPy/PDA composite mainly came from both the rough porous nanostructure and a large number of exposed hydrophilic groups such as ammonia hydroxyl groups on the surface of PDA.

PDA have astonishing adhesion ability, which can adhere to a variety of materials. We used the 3M tape to test the adhesion ability of different coatings with the substrate by tear test (Figure 4d). The result demonstrated that the deposited layer of PDA could even enhance the adhesion property of the PPy/PDA NWs coating with the Au surface compared with pure PPy NWs. After several instances of the tear test, PPy/PDA NWs coating still adhered to the substrate firmly with almost no material loss. Therefore, the enhancement of surface hydrophilicity and the increase of adhesion stability with substrates made PPY/PDA NWs a better coating material than pure PPy NWs.

The PPy/PDA NWs had good conductivity. The electrochemical property was measured by cyclic voltammetry in 0.9% NaCl solution (Figure 4e). Pure PDA was hardly conductive and had no obvious electrochemical activity. After PDA deposited, compared with pure PPy NWs, the electrochemical activity of PPy/PDA NWs did not decrease significantly. However, compared with pure PPy NWs, the redox peak of PPy/PDA NWs was slightly shifted, indicating that PDA was not only successfully modified on the surface of PPy, but also interacted with PPy.
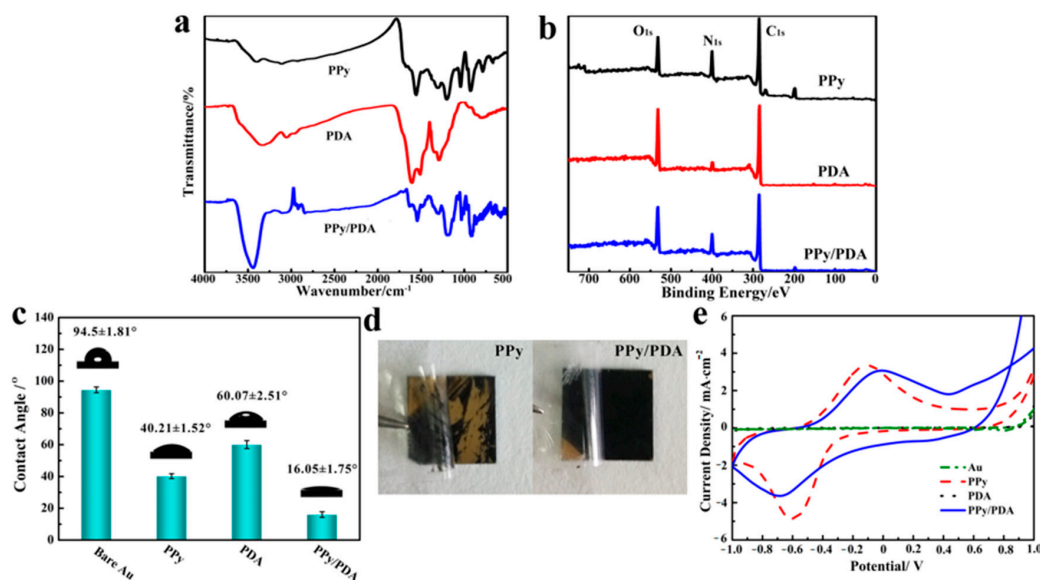

Figure 4. (**a**) FITR spectra of pure PPy NWs, PDA and PPy/PDA nanocomposite NWs. (**b**) XPS spectra of PPy NWs, PDA and PPy/PDA nanocomposite NWs. (**c**) The water contact angle of different material substrates. (**d**) The adhesion test of pure PPy NWs and PPy/PDA NWs. (**e**) Cyclic voltammogramms of different materials in 0.9% NaCl solution at the scan rate of 10 mV/s.

The above experiments demonstrated that via a two-step method, the PPy/PDA NWs nanocomposite coating was obtained. Compared with pure PPy NWs, PPy/PDA can effectively

increase the hydrophilicity of the coating and the firmness of adhesion with the substrate materials while retaining the excellent nanostructure, conductivity, and electrochemical activity. PDA has excellent biocompatibility and bioactivity. It has been confirmed that PDA can promote osteoblast cell adhesion and biomineralization [14]. We speculated that this nano-structured PPy/PDA NWs might have excellent promoting effect on osteogenesis than pure PDA and PPy.

3.2. Effect of PPy/PDA NWs Coating on MC3T3-E1 Activity

When contacting with materials, in the beginning 8–12 h, the main behavior of cells is to interact with the material and then adhere to the surface of material. The morphology, structure and chemical microenvironment of the materials all have significant effects on anchorage-dependent cell adhesion. SEM images showed that at the initial 12 h after cells were seeded, MC3T3-E1 cell could adhere and spread well on pure PPy NWs, PDA and PPy/PDA NWs coatings (Figure 5a). MTT test indicated that compared with bare Au, all modified coatings including pure PPy NWs, PDA and PPy/PDA NWs could promote the adhesion and proliferation of MC3T3-E1 cells, and the PPy/PDA NWs coating performed most effective facilitation (Figure 5b). SEM and fluorescence images detailed showed the morphology of MC3T3-E1 cells adhesion and spreading on the surface of different materials (Figure 5a). After 12 h, most cells on PPy NWs coating performed spindle and fibrous shape with some pseudo feet anchored on near PPy NWs. On the other hand, cells on the surface of PDA were flat and full spreading, and there were lots of pseudopods linked cells with each other, which proved that PDA can promote cell spreading better than PPy NWs, while MC3T3-E1 cells grew on PPy/PDA NWs coating were well spreading than pure PPy NWs. Most cells on PPy/PDA NWs surface were spreading flat, and pseudopodia filaments of cells were dispersed into surrounding nanowires and adhered closely to the substrate. Moreover, MC3T3-E1 cells were interconnected with each other through a large number of pseudopods. After 12 h of inoculation, the adherent cells entered the fast proliferative phase (Figure 5a,b). MC3T3-E1 cells on all substrates were grew well, and cells on PPy/PDA NWs coating had the fastest growth rate, which ensured that the PPy/PDA NWs coating had excellent biocompatibility and bioactivity and was more benefit for cell adhesion and proliferation than pure PPy NWs and PDA.

For the PPy/PDA NWs nanocomposite, the PDA deposition introduced abundant active functional groups on the inert surface of PPy, which facilitated early cell recognition and anchoring adhesion process. Moreover, the morphology of nanowires was closer to the natural extracellular matrix (ECM) morphology and the primary growth environment of osteoblasts, which significantly promoted the adhesion and proliferation of MC3T3-E1 cells on the surface. Therefore, the PPy/PDA NWs coating took the advantages of both nano morphology came from PPy NWs and excellent biological active inherited from PDA, and had the best value for cell adhesion and proliferation than pure PPy NWs and PDA.

In the procedure of culture osteoblasts for 14 days, it can be divided into three stages [36]. First, the adhesion between cells and matrix was mainly carried out within 12 h after cells were seeded. After 2–3 days, the cells entered the rapid proliferation stage. In this stage, large amounts of protein and DNA were synthesized. Finally, after 6–9 days, the cell proliferation basically stopped and began to enter the mineralization stage. At this stage, the metabolic activity of cells was still vigorous, and the activity of osteoblast markers represented by alkaline phosphatase (ALP) increased significantly, and osteoblasts began to enter differentiating and mature process.

The content of total protein in cells could be used to describe the proliferation and metabolic activity of cells. By testing the total protein content of MC3T3-E1 that cells grew on different coatings (Figure 5c), it could be found that the proliferation and metabolism activity of MC3T3-E1 cells growing on the surface of PPy NWs, PDA and PPy/PDA NWs coatings were all more vigorous than that of the control group (bare Au), and the cell on the PPy/PDA NWs coating maintained the highest protein content during the 14 days throughout, which indicated the PPy/PDA NWs coating could promote the cell rapid proliferation and metabolism activity than pure PPy NWs and PDA.
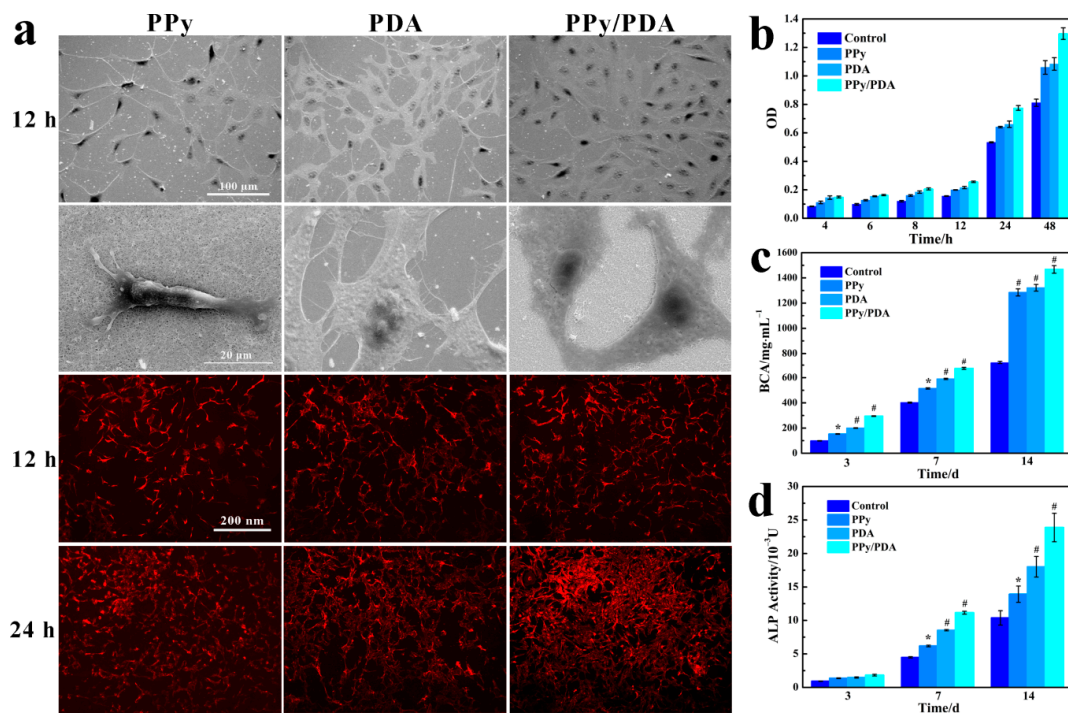
Figure 5. (**a**) SEM and fluorescence images of MC3T3-E1 cells on PPy NWs, PDA and PPy/PDA NWs cultured for 12 h and 24 h. (**b**) Proliferation of MC3T3-E1 cells on different coatings. (**c**) The protein content of MC3T3-E1 cells cultured on different coatings. (**d**) The ALP activity of MC3T3-E1 cells cultured on different coatings. * $p < 0.05$, and # $p < 0.01$.

The ALP activity, the early marker of osteogenic differentiation, could evaluate the osteogenic activity of MC3T3-E1 cells cultured on different coatings. As the result indicated (Figure 5d), at the initial stage of three days, the ALP activity of cells grown on four kind of coatings were all at low level without obvious difference. At this time, t cells were mainly in the rapid proliferation phase with low osteogenic activity. After 7 days, cells gradually entered the mineralization stage and the ALP activity in all group increased, and the PPy/PDA NWs group had the highest ALP activity. After 14 days, the advantage of ALP activity in PPy/PDA NWs group continued to expand, indicating that PDA/PPy NWs could significantly promote the mineralization and osteogenesis of MC3T3-E1 cells.

Above results demonstrated that the PPy/PDA NWs nanocomposite coating was not only helpful to the rapid adhesion of cells on the surface of materials, but also conducive the osteogenic activity for new bone formation.

3.3. Synergistic Effect of PPy/PDA NWs Coating with Electrical Stimulation on MC3T3-E1 Activity

In the process of bone formation and bone remodeling, electrical microenvironment around the bone cells occurs. Many studies confirmed that a small amount of electrical stimulation (ES) can significantly promote the proliferation and differentiation of osteoblasts at the cellular and tissue level [37,38]. PPy has good conductivity, and could be fabricated as a conductive coating to apply ES on cells sensitive to electrical signals. Our previous study have demonstrated that MC3T3-E1 cells shows better osteogenic activity on the surface of PPy coating with ES [39]. The PPy/PDA NWs was well maintained the excellent conductivity of PPy NWs layer, and performed better osteogenic differentiation activity than pure PPy NWs. Next, we used a self-made device to apply a constant current electrical stimulation (10 μA) to MC3T3-E1 cells through the PPy/PDA coating, and to study the synergistic effect of PPy/PDA NWs and ES working together on MC3T3-E1 cells.

After 12 h of the MC3T3-E1 cell culture, the constant ES was applied on cells for 2 h a day until 14 days. It could be seen that continuous ES can significantly increase the adhesion and proliferation

of MC3T3-E1 cell (Figure 6a), the number of MC3T3-E1 cells on PPy/PDA NWs coatings was almost doubled higher after ES was applied. Additionally, the total protein content and ALP activity tests relating to the proliferation and osteogenesis activity of MC3T3-E1 cells both revealed that the ES could promote the osteogenic differentiation of MC3T3-E1 cells (Figure 6b,c). It was noticeable that the total protein content and ALP activity value of MC3T3-E1 cells with ES at 7 days was very close to that of the cells without ES at 14 days, which proved that the PPy/PDA NWs coating together with ES addition could accelerate the cells entering the mature stage of osteogenic differentiation.
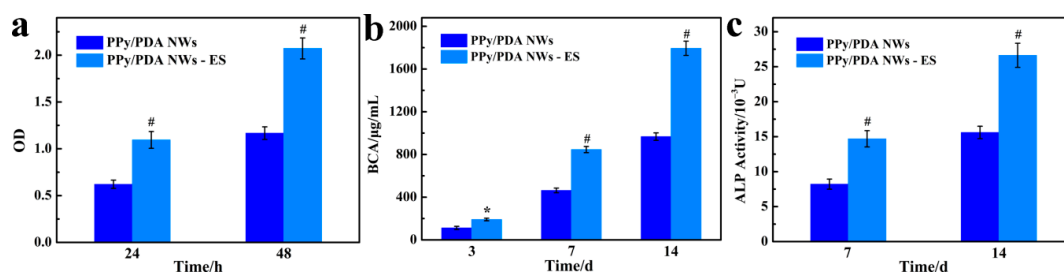
Figure 6. (**a**) The effect of ES on the proliferation of MC3T3-E1 cells on PPy/PDA NWs coating. (**b**) The effect of ES on the total protein content of MC3T3-E1 cells cultured on PPy/PDA NWs coating. (**c**) The effect of ES on the ALP activity of MC3T3-E1 cells cultured on PPy/PDA NWs coating. $* p < 0.05$, and $\# p < 0.01$.

4. Conclusions

We successfully fabricated the PPy/PDA NWs coating via a simple two-step method. By well controlling the depositing time of PDA within 5 h, the PPy/PDA NWs nanocomposite retained the nano morphology, conductivity, and electrochemical activity from the PPy NWs layer. Moreover, the introduction of the PDA deposition layer significantly improved the hydrophilicity and bioactivity of the material surface. In vitro experiments further proved that the PPy/PDA NWs composite coating had better biocompatibility and osteogenic differentiation ability than pure PPy NWs and PDA. MC3T3-E1 cells could quickly adhere and anchor on the surface of PPy/PDA NWs coating, and enter the proliferation and differentiation process. Furthermore, external applied ES with PPy/PDA NWs coating had the synergistic effect in stimulating the osteogenesis of MC3T3-E1 cell. Therefore, the PPy/PDA NWs composite is a potential coating with enhanced biocompatibility and biological activity in bone regeneration and repairing.

References

1. Wu, J.-G.; Chen, J.-H.; Liu, K.-T.; Luo, S.-C. Engineering antifouling conducting polymers for modern biomedical applications. *ACS Appl. Mater. Interfaces* **2019**, *11*, 21294–21307. [CrossRef] [PubMed]

2. Hackett, A.J.; Malmström, J.; Travas-Sejdic, J. Functionalization of conducting polymers for biointerface applications. *Prog. Polym. Sci.* **2017**, *70*, 18–33. [CrossRef]

3. Hardy, J.G.; Lee, J.Y.; Schmidt, C.E. Biomimetic conducting polymer-based tissue scaffolds. *Curr. Opin. Biotechnol.* **2013**, *24*, 847–854. [CrossRef] [PubMed]

4. Xia, L.; Wei, Z.; Wan, M. Conducting polymer nanostructures and their application in biosensors. *J. Colloid Interface Sci.* **2010**, *341*, 1–11. [CrossRef]

5. Boehler, C.; Oberueber, F.; Asplund, M. Tuning drug delivery from conducting polymer films for accurately controlled release of charged molecules. *J. Control Release* **2019**, *304*, 173–180. [CrossRef]

6. Jiang, S.; Sun, Y.; Cui, X.; Huang, X.; He, Y.; Ji, S.; Shi, W.; Ge, D. Enhanced drug loading capacity of polypyrrole nanowire network for controlled drug release. *Synth. Met.* **2013**, *163*, 19–23. [CrossRef]

7. Mihardja, S.S.; Sievers, R.E.; Lee, R.J. The effect of polypyrrole on arteriogenesis in an acute rat infarct model. *Biomaterials* **2008**, *29*, 4205–4210. [CrossRef]

8. Bu, Y.; Xu, H.; Li, X.; Xu, W.; Yin, Y.-X.; Dai, H.; Wang, X.-B.; Huang, Z.-J.; Xu, P.-H. A conductive sodium alginate and carboxymethyl chitosan hydrogel doped with polypyrrole for peripheral nerve regeneration. *RSC Adv.* **2018**, *8*, 10806–10817. [CrossRef]

9. Lee, J.Y.; Bashur, C.A.; Goldstein, A.S.; Schmidt, C.E. Polypyrrole-coated electrospun PLGA nanofibers for neural tissue applications. *Biomaterials* **2009**, *30*, 4325–4335. [CrossRef]

10. Harjo, M.; Torop, J.; Järvekülg, M.; Tamm, T.; Kiefer, R. Electrochemomechanical behavior of polypyrrole-coated nanofiber scaffolds in cell culture medium. *Polymers* **2019**, *11*, 1043. [CrossRef]

11. Hu, W.-W.; Hsu, Y.-T.; Cheng, Y.-C.; Li, C.; Ruaan, R.-C.; Chien, C.-C.; Chung, C.-A.; Tsao, C.-W. Electrical stimulation to promote osteogenesis using conductive polypyrrole films. *Mater. Sci. Eng. C* **2014**, *37*, 28–36. [CrossRef] [PubMed]

12. Zhou, Z.; Chen, J.; Zhou, L.; Tu, L.; Fan, L.; Zhang, F.; Dai, C.; Liu, Y.; Ning, C.; Du, J.; et al. Polypyrrole nanocones and dynamic piezoelectric stimulation-induced stem cell osteogenic differentiation. *ACS Biomater. Sci. Eng.* **2019**, *5*, 4386–4392. [CrossRef]

13. Hardy, J.G.; Sukhavasi, R.C.; Aguilar, D.; Villancio-Wolter, M.K.; Mouser, D.J.; Geissler, S.A.; Nguy, L.; Chow, J.K.; Kaplan, D.L.; Schmidt, C.E. Electrical stimulation of human mesenchymal stem cells on biomineralized conducting polymers enhances their differentiation towards osteogenic outcomes. *J. Mater. Chem. B* **2015**, *3*, 8059–8064. [CrossRef]

14. Zhou, T.; Yan, L.; Xie, C.; Li, P.; Jiang, L.; Fang, J.; Zhao, C.; Ren, F.; Wang, K.; Wang, Y.; et al. A mussel-inspired persistent ROS-scavenging, electroactive, and osteoinductive scaffold based on electrochemical-driven in situ nanoassembly. *Small* **2019**, *15*, 1805440. [CrossRef] [PubMed]

15. Cheng, S.; Wang, D.; Ke, J.; Ma, L.; Zhou, J.; Shao, H.; Zhu, H.; Liu, L.; Zhang, Y.; Peng, F.; et al. Improved in vitro angiogenic behavior of human umbilical vein endothelial cells with oxidized polydopamine coating. *Colloids Surf. B* **2020**, *194*, 111176. [CrossRef]

16. Waite, J.H. The adhesive proteins secreted by mussels are the inspiration behind a versatile approach to the surface modification of a wide range of inorganic and organic materials, resulting in the fabrication of multifunctional coatings for a variety of applications. *Nat. Mater.* **2008**, *7*, 8–9. [CrossRef]

17. Zhang, W.; Pan, Z.; Yang, F.K.; Zhao, B. A facile in situ approach to polypyrrole functionalization through bioinspired catechols. *Adv. Funct. Mater.* **2015**, *25*, 1588–1597. [CrossRef]

18. Zeng, X.; Luo, M.; Liu, G.; Wang, X.; Tao, W.; Lin, Y.; Ji, X.; Nie, L.; Mei, L. Polydopamine-modified black phosphorous nanocapsule with enhanced stability and photothermal performance for tumor multimodal treatments. *Adv. Sci.* **2018**, *5*, 1800510. [CrossRef]

19. Zhang, P.-B.; Hu, W.; Wu, M.; Gong, L.; Tang, A.; Xiang, L.; Zhu, B.; Zhu, L.-P.; Zeng, H. Cost-effective strategy for surface modification via complexation of disassembled polydopamine with Fe(III) ions. *Langmuir* **2019**, *35*, 4101–4109. [CrossRef]

20. Ponzio, F.; Bertani, P.; Ball, V. Role of surfactants in the control of dopamine–eumelanin particle size and in the inhibition of film deposition at solid–liquid interfaces. *J. Colloid Interface Sci.* **2014**, *431*, 176–179. [CrossRef]

21. Zhang, W.; Yang, F.K.; Pan, Z.; Zhang, J.; Zhao, B. Bio-inspired dopamine functionalization of polypyrrole for improved adhesion and conductivity. *Macromol. Rapid Commun.* **2014**, *35*, 350–354. [CrossRef] [PubMed]

22. Kim, S.; Jang, L.K.; Park, H.S.; Lee, J.Y. Electrochemical deposition of conductive and adhesive polypyrrole-dopamine films. *Sci. Rep.* **2016**, *6*, 30475. [CrossRef] [PubMed]

23. Pan, J.; Yang, M.; Luo, L.; Xu, A.; Tang, B.; Cheng, D.; Cai, G.; Wang, X. Stretchable and highly sensitive braided composite yarn@polydopamine@polypyrrole for wearable applications. *ACS Appl. Mater. Interfaces* **2019**, *11*, 7338–7348. [CrossRef] [PubMed]

24. Kim, S.; Jang, L.K.; Jang, M.; Lee, S.; Hardy, J.G.; Lee, J.Y. Electrically conductive polydopamine-polypyrrole as high performance biomaterials for cell stimulation in vitro and electrical signal recording in vivo. *ACS Appl. Mater. Interfaces* **2018**, *10*, 33032–33042. [CrossRef] [PubMed]

25. Zhang, W.; Zhou, Y.; Feng, K.; Trinidad, J.; Yu, A.; Zhao, B. Morphologically controlled bioinspired dopamine-polypyrrole nanostructures with tunable electrical properties. *Adv. Electron. Mater.* **2015**, *1*, 1500205. [CrossRef]

26. Xie, C.; Li, P.; Han, L.; Wang, Z.; Zhou, T.; Deng, W.; Wang, K.; Lu, X. Electroresponsive and cell-affinitive polydopamine/polypyrrole composite microcapsules with a dual-function of on-demand drug delivery and cell stimulation for electrical therapy. *NPG Asia Mater.* **2017**, *9*, 358. [CrossRef]

27. Wang, Z.; Zhou, L.; Yu, P.; Liu, Y.; Chen, J.; Liao, J.; Li, W.; Chen, W.; Zhou, W.; Yi, X.; et al. Polydopamine-assisted electrochemical fabrication of polypyrrole nanofibers on bone implants to improve bioactivity. *Macromol. Mater. Eng.* **2016**, *301*, 1288–1294. [CrossRef]

28. Tan, J.; Zhang, Z.; He, Y.; Yue, Q.; Xie, Z.; Ji, H.; Sun, Y.; Shi, W.; Ge, D. Electrochemical synthesis of conductive. superhydrophobic and adhesive polypyrrole-polydopamine nanowires. *Synth. Met.* **2017**, *234*, 86–94. [CrossRef]

29. Huang, J.; Wang, K.; Wei, Z. Conducting polymernanowire arrays with enhanced electrochemical performance. *J. Mater. Chem.* **2010**, *20*, 1117–1121. [CrossRef]

30. Debiemme-Chouvy, C. Template-free one-step electrochemical formation of polypyrrole nanowire array. *Electrochem. Commun.* **2009**, *11*, 298–301. [CrossRef]

31. Ma, F.-F.; Zhang, D.; Zhang, N.; Huang, T.; Wang, Y. Polydopamine-assisted deposition of polypyrrole on electrospun poly(vinylidene fluoride) nanofibers for bidirectional removal of cation and anion dyes. *Chem. Eng. J.* **2018**, *354*, 432–444. [CrossRef]

32. Lee, H.; Dellatore, S.M.; Miller, W.M.; Messersmith, P.B. Mussel-inspired surface chemistry for multifunctional coatings. *Science* **2007**, *318*, 426–430. [CrossRef] [PubMed]

33. Liu, S.; Pan, T.; Wang, R.; Yue, Y.; Shen, J. Anti-corrosion and conductivity of the electrodeposited graphene/polypyrrole composite coating for metallic bipolar plates. *Prog. Org. Coat* **2019**, *136*, 105237. [CrossRef]

34. Luo, R.; Tang, L.; Wang, J.; Zhao, Y.; Tu, Q.; Weng, Y.; Shen, R.; Huang, N. Improved immobilization of biomolecules to quinone-rich polydopamine for efficient surface functionalization. *Colloids Surf. B* **2013**, *106*, 66–73. [CrossRef] [PubMed]

35. Zangmeister, R.A.; Morris, T.A.; Tarlov, M.J. Characterization of polydopamine thin films deposited at short times by autoxidation of dopamine. *Langmuir* **2013**, *29*, 8619–8628. [CrossRef]

36. Qqarles, L.D.; Yohay, D.A.; Lever, L.W.; Caton, R.; Wenstrup, R.J. Distinct proliferative and differentiated stages of murine MC3T3-El cells in culture: An in vitro model of osteoblast development. *J. Bone Miner. Res.* **1992**, *7*, 683–692. [CrossRef]

37. Lirani-Galvão, A.P.R.; Chavassieux, P.; Portero-Muzy, N.; Bergamaschi, C.T.; Silva, O.L.; Carvalho, A.B.; Lazaretti-Castro, M.; Delmas, P.D. Low-intensity electrical stimulation counteracts the effects of ovariectomy on bone tissue of rats: Effects on bone microarchitecture, viability of osteocytes, and nitric oxide expression. *Calcif. Tissue Int.* **2009**, *84*, 502–509. [CrossRef]

38. Lirani-Galvão, A.P.R.; Lazaretti-Castro, M.; Portero-Muzy, N.; Bergamaschi, C.T.; Silva, O.L.; Carvalho, A.B.; Delmas, P.D.; Chavassieux, P. Is nitric oxide a mediator of the effects of low-intensity electrical stimulation on bone in ovariectomized rats? *Calcif. Tissue Int.* **2010**, *87*, 52–59. [CrossRef]

39. He, Y.; Wang, S.; Mu, J.; Dai, L.; Zhang, Z.; Sun, Y.; Shi, W.; Ge, D. Synthesis of polypyrrole nanowires with positive effect on MC3T3-E1 cell functions through electrical stimulation. *Mater. Sci. Eng. C* **2017**, *71*, 43–50. [CrossRef]